Reliability and Conflict-Aware Closed-Loop Multimodal Edge Framework for Landslide Early Warning: A Simulation-Based Algorithmic Evaluation

Tanzine Sharia Morshed
Dept. of Computer Science & Engineering
Jatiya Kabi Kazi Nazrul Islam University
Trishal, Mymensingh, Bangladesh
poushie171@gmail.com

Aparajita Dhar
Dept. of Computer Science & Engineering
Jatiya Kabi Kazi Nazrul Islam University
Trishal, Mymensingh, Bangladesh
praptydhar35@gmail.com

Hussain Anjum Ratul
Dept. of Computer Science & Engineering
Jatiya Kabi Kazi Nazrul Islam University
Trishal, Mymensingh, Bangladesh
haratul14@gmail.com

Mostafa Shakib
Dept. of Computer Science & Engineering
Jatiya Kabi Kazi Nazrul Islam University
Trishal, Mymensingh, Bangladesh
mostafashakib41@gmail.com

Md. Sujan Ali
Dept. of Computer Science & Engineering
Jatiya Kabi Kazi Nazrul Islam University
Trishal, Mymensingh, Bangladesh
sujan_cse@jkkniu.edu.bd

***Abstract*—This paper presents a reliability- and conflict-aware multimodal fusion framework for landslide early warning under sensor degradation. The framework combines rainfall, soil moisture, and simulated deformation signals and adjusts their contributions according to availability, range validity, temporal stability, and drift. Cross-modal disagreement is handled separately. Evaluation uses a real landslide inventory from 2001–2017 containing 434 records with 338 temporally usable dates from Rangamati, Bandarban, and Cox's Bazar, Bangladesh. A frozen chronological protocol reserves 2017 as the locked test period, which contains three reconstructed test episodes. Warning thresholds are selected only from validation data subject to a target constraint of ≤ 4 false alarms per month. On the locked test set, the proposed framework detects 2 of 3 episodes (66.7% recall; 95% CI [9.4%, 99.2%]), the same recall obtained by rainfall-only and conventional fusion, while reducing total false alarms from 68 and 61 to 59, respectively. Under simulated sensor degradation, recall remains 66.7% and total false alarms decrease to 48. Reliability diagnostics show reductions of 1.28 percentage points for soil moisture, 0.65 percentage points for deformation, and 2.38 percentage points for rainfall under the corresponding degradation conditions. The locked test set contains only three episodes, two of which share a calendar date, so the wide confidence interval and simulated deformation do not support claims of operational forecasting performance; the contribution is methodological and the evaluation protocol is fully reproducible.**

***Index Terms*—Landslide early warning, multimodal sensor fusion, reliability-aware fusion, conflict-aware fusion, edge computing, sensor degradation, false alarm constraint, closed-loop decision making.**

I. Introduction

Landslides are a recurring hazard in southeastern Bangladesh, particularly in the Chittagong Hill Tracts, where steep terrain and intense monsoon rainfall contribute to slope instability [1], [2]. Research in this area has mainly focused on susceptibility mapping and risk assessment [1]–[3]. Practical early-warning systems require continuous sensing, multimodal integration, and timely edge-based decision-making.

Rainfall, soil moisture, and ground deformation provide complementary information about changing slope conditions. Measurements from these sensors can nevertheless be affected by missing observations, invalid values, instability, and drift. A fixed-weight fusion scheme does not account for these changes in data quality and can allow unreliable modalities to affect warning decisions. Disagreement between modalities also requires separate treatment. Such disagreement may arise from response times, measurement noise, or localized variability and does not necessarily indicate a sensor fault or hazardous condition. The fusion strategy therefore distinguishes sensor reliability from disagreement among modalities.

Edge processing is relevant here: remote hill slopes may have unreliable network connectivity, and communication delays can exceed the available warning window. Field nodes must operate during network outages, with decisions made locally.

A. Scope and Framing

The study evaluates algorithmic robustness under controlled sensor degradation using a real inventory from Rangamati, Bandarban, and Cox's Bazar. The inventory contains 434 records from 2001–2017, of which 338 have precise dates suitable for temporal evaluation. Applying a 72-hour gap between records produces 16 temporally separated episodes. A chronological split assigns 10 episodes to development, 3 to validation, and 3 to a locked 2017 test set. Because deformation is simulated, only three test episodes are available,

979-8-3195-2804-9/26/$31.00 ©2026 IEEE

and two of these share a calendar date, the results describe controlled robustness rather than operational forecasting performance.

B. Contributions

The main contributions are:

(i) A reliability- and conflict-aware fusion framework that treats sensor reliability and cross-modal disagreement as separate quantities. This suppresses degraded modalities without treating sensor faults as hazard-related disagreement.

(ii) An evaluation protocol based on episode reconstruction and a frozen chronological test set. Thresholds are selected using pooled validation data subject to a validation-stage false-alarm constraint of ≤ 4 false alarms per month.

(iii) A reproducible empirical evaluation on the locked test set showing 66.7% episode recall (2 of 3 episodes), matching the baselines while reducing total false alarms from 68 to 59. Under degradation, recall remains 66.7% and total false alarms decrease to 48. Reliability diagnostics show reductions for degraded soil (1.28 pp), deformation (0.65 pp), and rainfall (2.38 pp).

The remainder is organized as follows: Section II reviews related work, Section III describes the framework, Section IV presents the experimental evaluation, and Section V concludes.

II. Literature Review

A. Landslide Susceptibility and Risk Assessment

Landslide studies in Bangladesh have examined terrain, environmental, and anthropogenic factors associated with spatial susceptibility [1]–[3]. Chowdhury *et al.* [1] evaluated machine-learning approaches for susceptibility mapping, while Sayeem *et al.* [3] considered slope units and spatial uncertainty. Sultana *et al.* [2] combined hazard and vulnerability indicators to assess landslide risk.

B. Multimodal Landslide Monitoring

Recent work has explored multiple sensing modalities for landslide monitoring and early warning. Gupta and Satyam [4] combined rainfall, soil moisture, and deformation measurements for real-time hydrogeotechnical modelling, whereas Guo *et al.* [5] used integrated monitoring to examine rainfall-induced slope failure. Soil moisture has also been identified as a complementary indicator for rainfall-induced landslide warning [6], [7]. Adaptive and IoT-based monitoring architectures have also been investigated for resource-aware monitoring and early detection [8], [9]. Although these approaches demonstrate the benefit of heterogeneous observations, they do not consistently distinguish individual modality reliability from inter-modal disagreement during fusion.

C. Reliability-Aware and Robust Multimodal Fusion

Recent multimodal sensing research has increasingly considered unreliable and degraded sensor measurements. Zuo *et al.* [10] incorporated multiple reliability indicators into multisensor fusion, using data-quality information to adjust individual modality contributions. Park *et al.* [11] examined resilient multimodal fusion under sensor failures and emphasized reliable predictions when sensing sources become unreliable.

Reliability and inter-modal disagreement represent different types of uncertainty. A modality may become unreliable because of missing observations, abnormal values, instability, or drift, while two individually valid modalities may disagree because they respond differently to the same physical process. This distinction is particularly relevant to landslide early warning, where rainfall, soil moisture, and deformation can exhibit different responses to environmental changes and sensor disturbances.

D. Research Gap

The literature shows substantial progress in landslide susceptibility assessment, multimodal monitoring, adaptive sensing, and reliability-aware fusion. However, these areas are often studied independently. In particular, limited work explicitly evaluates the joint treatment of individual modality reliability and cross-modal disagreement for landslide early warning under controlled sensor degradation. The interaction between robust multimodal fusion and edge resource constraints is also important because field deployments may face limited communication, computation, and sensing resources.

III. Proposed System Architecture

A. Overall Architecture

The proposed system is a closed-loop multimodal edge-warning framework that combines rainfall, soil-moisture, and deformation measurements. Each modality is converted into a bounded pressure score and passed to a reliability estimator based on missingness, range validity, temporal stability, and drift. Disagreement between individual modalities and a reliability-weighted consensus reduces the contribution of inconsistent observations.

The fused risk score is passed to a risk-state manager. Its threshold is selected during validation subject to the predefined false-alarm constraint. The manager assigns one of five states: LOW, MEDIUM, HIGH, CRITICAL, or SENSOR-CONFLICT. State-specific persistence and cooldown limit transient transitions and unstable warnings. The resulting state feeds back into monitoring behavior, forming a closed decision loop.

B. Multimodal Pressure Computation

Three sensing modalities are considered: rainfall (R), soil moisture (M), and deformation (D). Each modality is converted into a normalized pressure score in $[0, 1]$.

For rainfall, the pressure score combines recent 24-hour accumulation with an exponentially decayed antecedent rainfall index. Let $\mathrm{rain}(t)$ denote hourly rainfall:

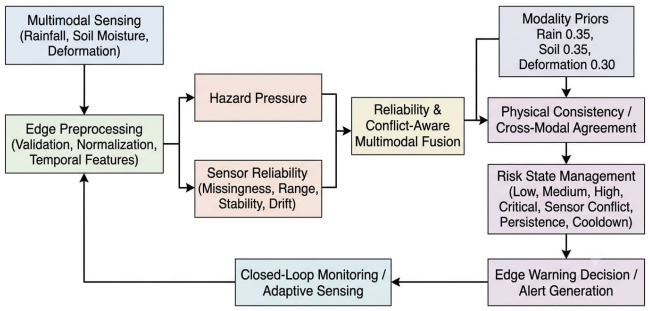


Fig. 1. Overall architecture of the proposed reliability- and conflict-aware multimodal edge-warning framework.

$$R_{24}(t) = \mathrm{clip}\left(\frac{\sum_{k=0}^{23} \mathrm{rain}(t-k) - 15}{60}\right), \tag{1}$$

$$A(t) = \mathrm{rain}(t) + 0.9A(t-1), \tag{2}$$

where $\mathrm{clip}(x) = \min(1, \max(0, x))$. The rainfall pressure is

$$s_R(t) = 0.6R_{24}(t) + 0.4\,\mathrm{clip}\left(\frac{A(t) - 10}{80}\right). \tag{3}$$

Soil-moisture pressure combines the current moisture level with its recent rate of change:

$$\begin{aligned} s_M(t) = 0.7\,\mathrm{clip}&\left(\frac{\mathrm{moisture}(t) - 0.25}{0.20}\right) \\ &+ 0.3\,\mathrm{clip}\left(10\,\overline{\Delta\mathrm{moisture}}_6(t)\right). \end{aligned} \tag{4}$$

Deformation pressure combines tilt magnitude, recent tilt change, and tilt acceleration:

$$\begin{aligned} s_D(t) =& 0.5\,\mathrm{clip}(100\,\mathrm{tilt_mag}(t)) \\ &+ 0.3\,\mathrm{clip}(200\,\overline{\Delta\mathrm{tilt_mag}}_6(t)) \\ &+ 0.2\,\mathrm{clip}(300\,\mathrm{tilt_acc}(t)). \end{aligned} \tag{5}$$

The normalization ranges (15, 60, 0.20, 80) are obtained from development-data percentiles. The sensitivity coefficients (10, 100, 200, 300) were fixed before evaluation.

The modality vector is

$$\mathbf{s}(t) = [s_R(t), s_M(t), s_D(t)], \tag{6}$$

which is passed to the reliability and fusion stages.

C. Modality Reliability Estimation

Reliability is estimated from four characteristics:

- **Missingness:** whether all required measurements are available at time t.
- **Range validity:** whether observations fall within the development-derived valid range.
- **Temporal stability:** a penalty for high short-term variance.
- **Drift:** persistent deviation between recent and longer-term observations.

$$r^m_{\mathrm{miss}}(t) = \mathbb{1}[\text{all required measurements available at } t], \tag{7}$$

$$r^m_{\mathrm{range}}(t) = \begin{cases} 1, & P^m_1 \le x_m(t) \le P^m_{99} \\ \exp\left(-\frac{|x_m(t) - P^m_{99}|}{P^m_{99} - P^m_1}\right), & x_m(t) > P^m_{99} \\ \exp\left(-\frac{|P^m_1 - x_m(t)|}{P^m_{99} - P^m_1}\right), & x_m(t) < P^m_1 \end{cases} \tag{8}$$

where P^m_1 and P^m_{99} are the 1st and 99th percentiles from development.

$$r^m_{\mathrm{stab},j}(t) = \exp\left[-\frac{\mathrm{Var}_{24}(x_j(t))}{V_{j,\mathrm{dev}} + \epsilon}\right], \tag{9}$$

$$r^m_{\mathrm{drift},j}(t) = \exp\left[-\frac{|\bar{x}^j_6(t) - \bar{x}^j_{72}(t)|}{\max(|\bar{x}^j_{72}(t)|, \sigma_{j,\mathrm{dev}}) + \epsilon}\right], \tag{10}$$

where $\sigma_{j,\mathrm{dev}}$ prevents hypersensitivity near zero.

Modality reliability is calculated using fixed weights:

$$c_m(t) = 0.15r^m_{\mathrm{miss}}(t) + 0.15r^m_{\mathrm{range}}(t) + 0.35r^m_{\mathrm{stab}}(t) + 0.35r^m_{\mathrm{drift}}(t). \tag{11}$$

TABLE I
RELIABILITY COMPONENTS AND WEIGHTS

Component	Purpose	Weight
Missingness	Detects unavailable measurements	0.15
Range validity	Detects observations outside limits	0.15
Temporal stability	Penalizes abnormal short-term variance	0.35
Drift	Penalizes persistent deviation	0.35

D. Reliability- and Disagreement-Aware Fusion

The modality priors are

$$(\pi_R, \pi_M, \pi_D) = (0.35, 0.35, 0.30). \tag{12}$$

A reliability-weighted consensus is calculated as

$$s_{\mathrm{consensus}}(t) = \sum_m \frac{c_m(t)\pi_m}{\sum_j c_j(t)\pi_j} s_m(t). \tag{13}$$

The contribution of each modality is then reduced according to its disagreement with the consensus:

$$\tilde{w}_m(t) = c_m(t)\pi_m \exp\left[-\lambda |s_m(t) - s_{\mathrm{consensus}}(t)|\right], \tag{14}$$

where $\lambda = 3.0$. The normalized weights and score are

$$w_m(t) = \frac{\tilde{w}_m(t)}{\sum_j \tilde{w}_j(t)}, \tag{15}$$

$$s_{\mathrm{fused}}(t) = \sum_m w_m(t) s_m(t). \tag{16}$$

Low reliability reflects poor data quality, whereas disagreement reflects inconsistency among available modalities. The conflict metric used to trigger the SENSOR-CONFLICT state is the minimum pairwise cross-modal agreement:

$$a(t) = \min_{m,n} \exp\left(-\lambda |s_m(t) - s_n(t)|\right), \tag{17}$$

where $a(t) < 0.30$ triggers the SENSOR-CONFLICT state.

E. Physical Consistency Adjustment

Short-term consistency between rainfall and soil-moisture responses is evaluated using the consistency score $C(t) \in [0, 1]$:

$$C(t) = \begin{cases} 0.7\frac{R_{\mathrm{inc}}(t)}{6} + 0.3\frac{M_{\mathrm{inc}}(t)}{3}, & R_{\mathrm{inc}}(t) > 0 \wedge M_{\mathrm{inc}}(t) > 0 \\ 0.5\frac{R_{\mathrm{inc}}(t)}{6}, & R_{\mathrm{inc}}(t) > 0 \wedge M_{\mathrm{inc}}(t) = 0 \\ 0, & \text{otherwise} \end{cases} \tag{18}$$

where $R_{\mathrm{inc}}(t)$ and $M_{\mathrm{inc}}(t)$ denote the number of hours during the past 6 hours with increasing rainfall and soil moisture, respectively.

The fused risk is adjusted as follows:

$$s_{\mathrm{adj}}(t) = \mathrm{clip}\left(\frac{s_{\mathrm{fused}}(t)[1 + 0.30C(t)]}{1.30}\right). \tag{19}$$

Normalization by 1.30 preserves the $[0, 1]$ bounds.

F. Risk-State Management

The adjusted score is mapped to an operational state using threshold θ. The threshold is selected exclusively from validation data subject to the false-alarm constraint.

TABLE II
RISK-STATE MAPPING AND WARNING POLICY

State	Score Condition	Warning	Policy
LOW	$s < 0.7\theta$	No	Normal monitoring
MEDIUM	$0.7\theta \le s < \theta$	No	Increased monitoring
HIGH	$\theta \le s < 1.2\theta$	Yes	Warning state
CRITICAL	$s \ge 1.2\theta$	Yes	Critical warning
SENSOR-CONFLICT	$a < 0.30$	Yes	Conflict warning

Persistence and cooldown depend on the warning state, limiting repeated transitions caused by short-lived fluctuations.

G. Frozen Configuration and Processing

All parameters are fixed before evaluation on the locked test set. Random seeds, software versions, configuration files, and the code repository are listed in the reproducibility subsection (Section IV).

Deformation is simulated; labels come from the real inventory. The synthetic deformation generator and the degradation injection procedure are documented in Section IV-B. Normalization constants (Eqs. 1–5) were derived from development-data percentiles; sensitivity coefficients, reliability weights, modality priors, $\lambda = 3.0$, conflict threshold 0.30, persistence, and cooldown were fixed as design choices; only the state threshold θ was selected from validation data under the ≤ 4 FA/month constraint.

IV. EXPERIMENTAL EVALUATION

A. Dataset and Evaluation Protocol

The evaluation uses a real landslide inventory from Rangamati, Bandarban, and Cox's Bazar. Of 730 records, 722 have valid dates and 434 fall within the study regions. Exact and corrected dates yielded 338 temporally usable records. Year-only records were excluded because their timing is insufficiently precise for episode reconstruction.

Chronological splitting of the 16 episodes produced 10 development, 3 validation, and 3 test episodes. The locked 2017 test set contains one Rangamati episode and two Bandarban episodes; Cox's Bazar has no test episode.

Hourly rainfall and soil moisture were obtained from Open-Meteo; deformation was generated synthetically. Soil drift, deformation-noise bursts, and rainfall degradation were injected into the test streams. Three methods were evaluated: rainfall-only, conventional fixed fusion, and the proposed reliability- and conflict-aware fusion. Thresholds were selected on validation data under a constraint of ≤ 4 false alarms/month and frozen for testing. The early-warning window was 24 h. A false alarm is defined as a HIGH, CRITICAL, or SENSOR-CONFLICT state transition occurring outside the 24 h early-warning window of any labeled episode; transitions within the cooldown period are suppressed and not counted. The rate is $\mathrm{FA/month} = (N_{\mathrm{FA}}/D_{\mathrm{eval}}) \times 30.44$, where D_{eval} is the evaluated period in days.

TABLE III
DATASET CONFIGURATION

Configuration	Value
Study regions	3
Inventory records	730
Primary usable records	338
Reconstructed episodes	16
Development / Validation / Test	10 / 3 / 3
Episode gap	72 h
Early-warning window	24 h
Validation FA/month constraint	4
Test period	2017

B. Synthetic Deformation and Degradation Settings

Deformation was generated synthetically because no synchronized historical deformation record was available. The generator combines a slow baseline oscillation, a logistic ramp activated only within 24 h before each labeled episode, additive Gaussian noise ($\sigma = 0.006$), and a random-walk drift.The generator uses a fixed seed of 244 (derived from a base seed of 42); the same stream is used for all methods. Landslide labels come exclusively from the real inventory; deformation is not used to define labels.

Three degradation types were injected into the test streams only. Development and validation streams were not degraded. Onsets and magnitudes were frozen before test evaluation (seed = 850). Table IV lists the parameters.

TABLE IV
DEGRADATION PARAMETERS (TEST STREAMS ONLY)

Type	Magnitude	Timing
Soil drift	Ramp to $+0.10$ VWC	First half of test
Soil noise	$\sigma = 0.02$	Full test period
Soil spikes	5% of points, ± 0.05	Random
Deformation bursts	$10\times$ baseline noise	5 bursts, 10–20 h
Rainfall under-catch	Ramp to $0.5\times$	Full test period
Rainfall noise	$\sigma = 0.01$	Full test period

C. Locked Test Performance

The locked 2017 test set contains three temporally separated episodes. Each method detects two episodes, giving 66.7% recall (95% CI: [9.4%, 99.2%]). Under clean conditions, the proposed method reduces false alarms to 59, compared with 68 for rainfall-only and 61 for conventional fusion. Under degradation, false alarms decrease to 48. Test-period false alarms are reported separately from the validation constraint.

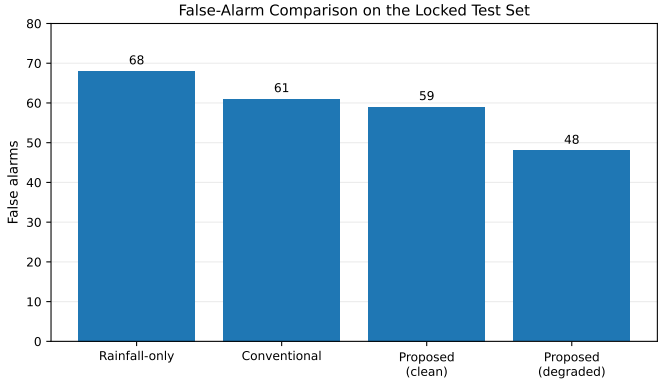


Fig. 2. False-alarm comparison on the locked 2017 test set (600 dpi; vector version in supplementary material).

D. Statistical Power and Reporting Scope

The locked test set contains three episodes, two of which occur on the same calendar date (2017-06-13) in different districts. The effective number of distinct event dates is therefore two, yielding a 95% confidence interval of [9.4%, 99.2%] for recall. This interval is wide and should be interpreted with caution. Cross-validation is not used as a primary performance estimate because the reconstructed episodes are clustered temporally and geographically, while several leave-one-episode-out training/validation configurations contain no positive events. Such folds do not provide a meaningful basis for event-recall threshold selection. Performance is therefore reported on the predefined locked 2017 test set, with the small test sample explicitly reflected in the confidence interval. Both the locked-test results and the reliability diagnostics are fully reproducible.

E. Novelty Summary

Table V compares the design of the proposed framework with two baselines: a rainfall-only thresholding approach following regional soil-moisture/rainfall early-warning practice [6], [7], and a conventional fixed-weight multimodal fusion scheme [4], [5], [8], [9]. The framework explicitly combines reliability estimation, conflict-aware fusion, physical consistency adjustment, and a closed-loop state manager for multimodal landslide early warning under a frozen false-alarm constraint.

TABLE V
DESIGN COMPARISON OF WARNING STRATEGIES

Feature	Rainfall-only	Conventional	Proposed
Multimodal fusion	No	Yes	Yes
Reliability estimation	No	No	Yes
Conflict handling	No	No	Yes
Physical consistency	No	No	Yes
State persistence	No	No	Yes
Cooldown mechanism	No	No	Yes
Closed-loop management	No	No	Yes
Degradation evaluation	Limited	No	Yes

F. Reliability and Degradation Analysis

The reliability measures respond selectively to the imposed degradation. Mean rainfall, soil, and deformation reliability changes from 0.5998, 0.6147, and 0.4737 under clean conditions to 0.5998, 0.6019, and 0.4672 under degradation. Additional rainfall degradation reduces rainfall reliability to 0.5760. The lower degraded FA count reflects reliability down-weighting, not improved sensing.

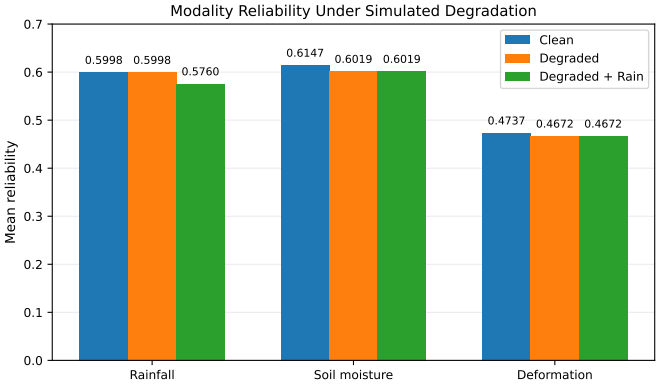


Fig. 3. Mean modality reliability under clean and degraded conditions (600 dpi; vector version in supplementary material).

Thresholds were selected from validation data under the validation-stage false-alarm constraint, as shown in Table VI. All thresholds were frozen before test evaluation.

TABLE VI
VALIDATION THRESHOLD SELECTION

Method	Threshold	Early Recall	FA/month
Rainfall-only [6], [7]	0.498599	33.33%	2.00
Conventional [4], [5], [8], [9]	0.341987	33.33%	2.83
Proposed	**0.324832**	**33.33%**	**3.02**

Because the locked test set contains only three episodes, the results reflect algorithmic robustness under controlled conditions.

V. Conclusion, Limitations, and Future Work

A. Conclusion

This study presented a reliability- and conflict-aware multimodal edge framework for landslide early warning using rainfall, soil moisture, and simulated deformation. The framework combines reliability-based weighting, disagreement-aware fusion, physical consistency adjustment, and warning-state persistence and cooldown.

Of 434 records, 338 had precise temporal information. A 72-hour gap produced 16 episodes, divided chronologically into 10 development, 3 validation, and 3 locked test episodes.

On the locked test set, the proposed framework detected 2 of 3 episodes (66.7%), matching rainfall-only and conventional fusion, while reducing false alarms from 68 and 61 to 59. Under simulated degradation, recall remained 66.7% and false alarms decreased to 48.

The framework was developed and validated on a 16-episode inventory; performance is reported on the locked 3-episode test set. However, the three-episode test set and simulated deformation limit operational forecasting claims.

B. Limitations

The main limitations are:

1) **Small test sample:** Only 3 test episodes were available in the locked chronological split, resulting in a wide 95% recall confidence interval of [9.4%, 99.2%].
2) **Simulated deformation and degradation:** Deformation and sensor faults were simulated, limiting real-world validity.
3) **Temporal uncertainty:** Year-only records were excluded from the primary evaluation.
4) **Parameter dependence:** Reliability parameters, modality priors, disagreement settings, persistence, cooldown, and thresholds were fixed and may require recalibration for different environments.
5) **Regional coverage:** Cox's Bazar contained no test episodes under the chronological split, limiting assessment of regional generalization.

C. Future Work

Future work should evaluate the framework with real multi-sensor observations and larger inventories containing precise event times. The degradation model should also cover missing data, saturation, calibration bias, nonlinear drift, communication failures, and correlated faults.

Additional studies should include other regions and modalities, such as groundwater level and GNSS. Reliability and fusion parameters could be learned from field data. Explainable warning outputs could also identify the modality, reliability condition, or conflict responsible for each decision.

Overall, this study provides a reproducible framework for evaluating reliability-aware multimodal fusion under a false-alarm constraint using a real inventory. The contribution is primarily methodological; larger-scale field validation with real deformation sensors is still required to establish practical forecasting effectiveness.

References

[1] M. S. Chowdhury, M. N. Rahman, M. S. Sheikh, M. A. Sayeid, K. H. Mahmud, and B. Hafsa, "Gis-based landslide susceptibility mapping using logistic regression, random forest and decision and regression tree models in chattogram district, bangladesh," *Heliyon*, vol. 10, no. 1, p. e23424, 2024.

[2] N. Sultana, S. Tan, and M. F. Hossen, "Landslide risk assessment by integrating hazards and vulnerability indices in southeast bangladesh," *International Journal of Disaster Risk Reduction*, vol. 114, p. 104991, 2024.

[3] M. A. A. Sayeem, P. R. Nobin, and R. B. Rahman, "Slope-unit based landslide susceptibility mapping using explainable ensemble machine learning and spatial uncertainty analysis in the chittagong hill tracts, bangladesh," *Remote Sensing Applications: Society and Environment*, vol. 42, p. 102091, 2026.

[4] K. Gupta and N. Satyam, "Integrating real-time sensor data for improved hydrogeotechnical modelling in landslide early warning in western himalaya," *Engineering Geology*, vol. 338, p. 107630, 2024.

[5] J. Guo, F. Meng, and J. Guo, "Gradual failure of a rainfall-induced creep-type landslide and an application of improved integrated monitoring system: A case study," *Sensors*, vol. 24, no. 22, p. 7409, 2024.

[6] M. Pavanello, M. Bordoni, V. Vivaldi, M. Reguzzoni, A. Tamburini, F. Villa, and C. Meisina, "Low-cost sensors for the measurement of soil water content for rainfall-induced shallow landslide early warning systems," *Water*, vol. 16, no. 22, p. 3244, 2024.

[7] A. Wicki, P. Lehmann, C. Hauck, S. I. Seneviratne, P. Waldner, and M. Stähli, "Assessing the potential of soil moisture measurements for regional landslide early warning," *Landslides*, vol. 17, no. 8, pp. 1881–1896, 2020.

[8] X. Dai, Z. Liu, Q. Liu, and L. Cheng, "Rainfall-adaptive landslide monitoring framework integrating flac3d numerical simulation and multi-sensor optimization: A case study in the tianshan mountains," *Sensors*, vol. 25, no. 17, p. 5433, 2025.

[9] M. H. Antora, F. N. Rahman, R. Debnath, A. A. Ahmed, and M. J. B. Alam, "A scalable hydrology-informed monitoring system for early detection of slope failures using iot and ml," *IEEE Access*, vol. 14, pp. 10 735–10 759, 2026.

[10] K. Zuo, X. Li, X. Li, K. Wang, T. Gao, and T. Shen, "Multi-sensor fusion with triple reliability evaluation for human activity recognition," *Measurement*, vol. 257, p. 118580, 2026.

[11] K. Park, Y. Kim, D. Kim, and J. W. Choi, "Resilient sensor fusion under adverse sensor failures via multi-modal expert fusion," in *Proceedings of the IEEE/CVF Conference on Computer Vision and Pattern Recognition (CVPR)*, 2025, pp. 6720–6729.